Potential of electric mobility as service to the grid in renewable energy hubs

Cédric Terrier[a], Luise Middelhauve[a] and François Maréchal[a]

[a] *Industrial Processes and Energy Systems Engineering, École Polytechnique Fédérale de Lausanne, Sion, Switzerland, cedric.terrier@epfl.ch[CA]*

Abstract:

The electrification of private mobility is becoming a popular solution to reduce the reliance on fossil fuels. However, uncontrollable charging of a large electric vehicle fleet challenges the distribution grid due to transmission bottlenecks, voltage limit violation or excessive wearing. In contrast, the additional storage capacities represent a potential flexibility service for grid operators. Therefore, the optimal integration of electric vehicles in urban multi-energy systems is key to minimize the power grid reliance and to maximize the self-consumption of renewable energy resources. The aim of this paper is to integrate electric mobility in the concept of a renewable energy hub formulated at the district scale. The model is a mixed-integer linear programming problem, and the Dantzig-Wolfe decomposition is applied to reduce the computational time. The electric vehicles are considered as controllable reserves offering services to grid operators. An electric mobility integration of 20% is considered. The results demonstrated the economic feasibility of electric mobility integration where services to the grid allowed for a 70% reduction in charging costs and a 50% reduction in global warming potential. The grid services allowed for an increase in self-consumption (70% with respect to 55%) and the charging of the vehicle was managed by up to 82% of renewable electricity. The optimal battery management of the vehicles demonstrated peak load reductions and promoted a grid-aware design of the renewable energy hub.

Keywords:

Decomposition; Electric mobility; Grid integration; Multi-objective optimization; Renewable energy hub.

Acronyms:

EVs: electric vehicles; V2G: vehicle to grid; PV: photovoltaic; MOO: multi-objective optimization; MP: master problem; SPs: subproblems; SoC: state of charge; KPI: key performance indicators; SC: self-consumption; SS: self-sufficiency; PVP: PV penetration; GWP: global warming potential

1. Introduction

The private transportation and the building sectors are major contributors to the global warming. They respectively account for 23% [1] and 19% [2] of the annual greenhouse gas emissions. To reduce the global warming potential impact, these sectors are expected to electrify rapidly. In 2050, the share of electricity will reach 50% to 60% in the transportation sector and 73% for the residential sector [1]. These values should be compared to the actual ones of respectively 1% and 32%. This fast-paced electrification is not without any consequences for the grid utility. The combination of high electric demands and uncontrollable grid imports is expected to cause transformer overloads, grid bottlenecks and to affect the power quality of the grid [3]. In addition, a high reliance on intermittent renewable energies in the low voltage grid also generates export power peaks challenging the transformer capacities. Versatile solutions have been proposed to prevent large grid reinforcement investments. A popular one is to take advantage of the storage capacity from the electric vehicles (**EVs**) to furnish grid services. Another solution is to maximize the self-consumption (**SC**) of the onsite generated electricity to minimize electricity exports to the grid. This, however, requires an optimal integration of the EVs within the energy system.

The concept of grid services with EVs lies within the vehicle to grid (**V2G**) framework. The consumers become prosumers by sharing the storage capacities of the EVs with the community and grid operators. Numerous studies reviewed the different grid service possibilities [4–6]. At the second time scale, the regulation up and down balances the grid demand and supply [4]. From the minute to the hour levels, the grid service can take the form of spinning and non-spinning reserves [4, 5]. Active power support can also be supplied to flatten the demand profile using peak shaving and load leveling [6]. Last but not least, EVs have a strong potential to support renewable integration by mitigating intermittences [6].

The type of charging control determines which grid service can be supplied. With unconstrained charging, the EVs are charged once plugged-in. This represents the worse case scenario since it disallows any grid service and is the source of grid instabilities [5]. With delayed charging control the charging is shifted to the periods when the electricity demand is low, usually during the night [4]. Finally, the smart charging strategy provides the highest charging control to the fleet operators. It takes the form of a direct control or an indirect one using price signals [4]. Indirect control has a higher degree of acceptances compared to a direct control since it provides more flexibility to the EV owners. Beside these control strategies, the V2G concept can be unidirectional and bidirectional. In the former, the fleet operator only controls the charging aspect while the latter also allows power supply from the EVs to the grid. Therefore, the grid services are improved with a bidirectional approach. Regardless the type of grid service and control, the performance and lifetime of the batteries are affected by their increased usage. Therefore, incentives should be sufficient to compensate for the reduction of performances and EV access flexibility. An interesting approach relying on car-sharing has been proposed by Brinkel et al. to handle this issue [7].

Table 1: Literature review on the integration of electric mobility. The papers are analysed based on the scope of the research. Many use aggregation or pre-selection of the energy system to simplify the models.

scale	solving strategy	multi-energy	renewable integration	grid-aware	MOO	reference
building	simulation	✗	✓	✗	✗	[8]
building	pre-selection	✗	✓	✓	✗	[9]
region	pre-selection + decomposition	✗	✓	✓	✗	[10]
building	pre-selection	✗	✓	✓	✗	[11]
building	pre-selection + variable unit sizes	✓	✓	✓	✗	[12]
district	pre-selection	✓	✗	✗	✗	[13]
district	pre-selection	✗	✓	✓	✗	[7]
district	pre-selection	✗	✓	✓	✓	[14]
district	pre-selection	✗	✓	✓	✗	[15]
district	simulation	✗	✓	✗	✗	[16]
district	aggregation	✗	✓	✗	✗	[17]
district	aggregation	✗	✓	✓	✗	[18]
district	aggregation	✓	✓	✗	✓	[19]
region	aggregation	✓	✓	✗	✓	[20]
district	pre-selection	✗	✓	✗	✗	[21]
district	decomposition	✓	✓	✓	✓	This paper

The literature analysed (Table 1) revealed many synergies between EVs and the onsite generation of renewable energy. The joint integration reduces the electricity curtailment, enhances the SC and decreases the EV charging costs [22]. It minimizes both the cost and emission objectives that are traditionally two competing objectives. In the residential sector, the integration of EVs with photovoltaic (**PV**) units is especially relevant due to the spatial proximity between the two technologies [4]. At the building level, Ritte et al. [8] simulated the synergies between EVs and onsite electricity generation. The results showed a share of renewable energy consumption in the EVs reaching 40%. However, the results were highly sensitive on the driver habits. While the SC is maximal for short-distance commuters, it is negligible for the long-distance ones since the peak of electricity generation usually happens while the EVs are not plugged-in [22]. Therefore, there is an interest to analyse the energy system at the district or regional scales. Increasing the spatial dimension enhances the probability of presence of plugged-in EVs. In addition, it allows a better consideration of the limitations from the grid infrastructure. Under this framework, Brinkel et al. [14] developed a multi-objective optimization (**MOO**) model to optimize the costs and emissions of a low voltage residential grid with 26 EV charging stations. They showed a cost reduction of 32% with controlled charging with respect to an uncontrolled strategy. The SC was increased and the grid reinforcement needs were minimized. Soares et al. [15] minimized the operating costs of a 27-bus microgrid and demonstrated a 70% cost reduction with controlled charging. A simulation of a university microgrid with EVs and PV units was performed by Zhang et al. [16]. The controlled charging was increasing the SC by 50% and was reducing the grid imports by 73%.

Despite the extensive literature existing on the topic, only few considered a holistic framework. From Table 1, most of the research analysed is pre-selecting the design of the energy system and is focusing only on the operations of the system. It is especially important to consider the design as a variable since a high share of EVs might change the investment decisions regarding the PV and battery capacities. What is more, the multi-energy nature of the energy system is neglected in many cases. Considering the energy system as a renewable energy hub favors extra synergies between the different energy fluxes. For example, EVs have the potential to enhance the SC using the heat pumps. Therefore, based on the literature review, we aim to contribute to the following research points:

- Optimal integration of electric mobility in a renewable energy hub at the district scale considering the multi-energy dimension
- Integration of the grid services from the EVs within the renewable energy hub
- Demonstration of the feasibility and synergies between PV units and EVs
- Multi-objective optimization framework and grid constraint consideration

2. Methodology

2.1. Renewable energy hub formulation

2.1.1. Overview

The model is formulated within the framework of a renewable energy hub, as defined by Middelhauve et al. [23]. A renewable energy hub is a multi-energy system that maximizes the self-consumption of onsite renewable energy. It is considered at the district scale, with optimally interconnected buildings. The objectives of a renewable energy hub are the optimal design of the energy system, considering investment decisions in energy units, and its optimal operation from the perspective of the whole district.

Considered energy demands are the demand for space heating, hot water and electricity. Each building is connected to the fresh water, the electricity and the natural gas grid. The integer variables decide for the installation of a unit in the renewable energy hub. In each building, the options to choose from are thermal and electrical energy conversion units. It includes for the thermal units air water heat pumps, gas boilers, electrical heaters and storage units in form of two thermal tanks, one for each thermal demand. Electricity storage is available at the district scale and modelled as lithium batteries. The main source of renewable electricity are PV units, which can be installed on the roof and facades of buildings. The orientation of the PV units is a decision variable and modelled as explained in [23].

The main constraints are the energy and mass balances and the heat cascade. Since the formulation is at the district scale, the electricity and natural gas balances are defined at the building and district scales. The thermal balance and heat cascade are modelled at the building scale, with the option to pre-heat the building at times of surplus electricity from the PV panels. The model encompasses four main sets: the unit U, the typical period P, the timestep of the typical period T and the building B. To reduce computational burdens, two methods are applied. The temporal resolution is reduced by clustering the time series into typical and extreme operating periods. The K-medoids clustering algorithm is used for that. Then, the spatial resolution is handled by applying the Dantzig-Wolfe decomposition method.

2.1.2. Objective functions

Three main objective functions are applied (Eq.1a to 1e). In the following equations, the variables are set in **bold** characters and the parameters in light characters. The total expenses (TOTEX, Eq. 1a) correspond to the sum of the operating cost (OPEX) and capital costs (CAPEX). The OPEX (Eq. 1b) is the annual sum of the costs and revenues associated with the exchange of energy with the electricity and natural gas utilities. The retail tariff of electricity and gas are respectively $c^{el,+}$ and $c^{ng,+}$ and the feed-in tariff of electricity is $c^{el,-}$. The variable E^{tr} corresponds to the annual electricity exchange at the transformer level. The term $H^{gr,+}$ is the equivalent of $E^{tr,+}$ for the natural gas. The CAPEX (Eq. 1c) correspond to the investments and replacement costs of the units annualized with an interest rate i over the n years horizon. The investment costs C^{inv} are function of the decision to install a unit (y^u) and of the size installed (f^u). These costs are linearized with the coefficients $i^{c1,u}$ and $i^{c2,u}$ with a bare modulus b^u [24]. Certain units have a lifetime l_u lower than the horizon n considered. The cost to replace them (C^{rep}) depends on the number of replacements R over the horizon n.

$$\boldsymbol{TOTEX} = \boldsymbol{OPEX} + \boldsymbol{CAPEX} \tag{1a}$$

$$\boldsymbol{OPEX} = c^{el,+} \cdot \boldsymbol{E^{tr,+}} - c^{el,-} \cdot \boldsymbol{E^{tr,-}} + c^{ng,+} \cdot \boldsymbol{H^{gr,+}} \tag{1b}$$

$$\boldsymbol{CAPEX} = \frac{i(1+i)}{(1+i)^n - 1}(\boldsymbol{C^{inv}} + \boldsymbol{C^{rep}}) \tag{1c}$$

$$\boldsymbol{C^{inv}} = \sum_{u=1}^{U} b^u \cdot (i^{c1,u} \cdot \boldsymbol{y^u} + i^{c2,u} \cdot \boldsymbol{f^u}) \tag{1d}$$

$$\boldsymbol{C^{rep}} = \sum_{u=1}^{U} \sum_{r=1}^{R} \frac{1}{(1+i)^{r \cdot l_u}} \cdot (i^{c1,u} \cdot \boldsymbol{y^u} + i^{c2,u} \cdot \boldsymbol{f^u}) \tag{1e}$$

MOO is performed with the OPEX and CAPEX using epsilon constraints. One objective is minimized while the other objective is lower bounded by an ϵ-value. Pareto fronts are built by alternating the objective constrained with the objective optimized and by varying the ϵ-values.

2.1.3. Electricity balance and grid constraint

The formulation being at the district scale, the electricity exchange is allowed between the building (Eq. 2a). This electricity sharing decreases the costs since the operating costs are evaluated on the transformer level. In addition, it reduces the burdens on the transformer of the district, that have a limited capacity $\dot{E}^{tr,max}$. Constraint 2b is applied to consider the transformer capacity in the model.

$$\sum_{b \in \mathrm{B}} (\boldsymbol{\dot{E}^{gr,+}_{b,p,t}} - \boldsymbol{\dot{E}^{gr,-}_{b,p,t}}) \cdot d_p \cdot d_t = \boldsymbol{E^{tr,+}_{p,t}} - \boldsymbol{E^{tr,-}_{p,t}} \qquad \forall p \in \mathrm{P}, \quad \forall t \in \mathrm{T} \tag{2a}$$

$$\boldsymbol{\dot{E}^{tr,\pm}_{p,t}} \leq \dot{E}^{tr,max} \qquad \forall p \in \mathrm{P}, \quad \forall t \in \mathrm{T} \tag{2b}$$

2.2. Decomposition

The methodology behind the decomposition is explained in detail in [23] and is summarized in the following. Due to the network structure of the district renewable energy hub, the resolution time has an exponential growth with respect to the size of the system. Therefore, the formulation of the energy system is decomposed into smaller problems. A master problem (**MP**) and several sub problems (**SPs**) are built. All the linking constraints are included in the MP. They correspond to the electricity balance 2a and transformer constraint 2b since they are linking the building energy systems. The MP receives design proposals from the SPs, applies the objective function, selects the best designs and calculates the dual values of the linking constraints. These values are sent to the SPs as price signals. The SPs are formulated at the building scale. Their purpose is to furnish design proposals to the MP. The dual values, or price signals, of the MP are incorporated in the objective function of the SPs to influence the optimization. The optimization iterates by solving alternatively the SPs and the MP and terminates when it reaches optimality or another stopping criteria, such as the maximum iterations or maximum CPU time allowed.

2.3. Electric vehicle model

The EVs are modelled at the district scale with a top down approach. A bidirectional control is applied between the EVs and the microgrid of the district. The EVs are considered as one central battery with a varying capacity over the day. This capacity depends on the ratio of EVs being plugged-out at each time step (α). The model contains three type of constraints: the electricity balances (Eq. 3a-3c), the charging/discharging constraints (Eq. 4a-4f) and the cyclicity constraints (Eq. 5a-5b). The costs associated to the EVs are the operating costs of the electricity consumption. The capital costs of the EVs and substations are not considered.

The overall stored energy is given by the variable E^{ev} and is the sum of the energy stored in the EV being plugged-out $E^{ev,out}$ and plugged-in $E^{ev,in}$ (Eq. 3a). When the EVs are plugged-out, they cannot exchange electricity with the grid. Therefore, the energy balance 3b only considers the electricity demand for travelling, $E^{ev,displ}$ and the self-discharge of the battery determined by the self-discharge rate η^{self}. On the other side, the EVs plugged-in can furnish grid services by exchanging electricity with the grid (Eq. 3c). The power supplied to and extracted from the EVs are respectively $\dot{E}^{ev,+}$ and $\dot{E}^{ev,-}$. Both values are subject to the charging and discharging efficiencies η^{ch} and η^{dis}.

$$\boldsymbol{E^{ev}_{p,t}} = \boldsymbol{E^{ev,out}_{p,t}} + \boldsymbol{E^{ev,in}_{p,t}} \qquad \forall p \in \mathrm{P}, \quad \forall t \in \mathrm{T} \tag{3a}$$

$$\boldsymbol{E^{ev,out}_{p,t}} = \eta^{self} \cdot \boldsymbol{E^{ev}_{p,t-1}} \cdot \alpha_{p,t} - E^{ev,displ.}_{p,t} \qquad \forall p \in \mathrm{P}, \quad \forall t \in \mathrm{T} \tag{3b}$$

$$\boldsymbol{E^{ev,in}_{p,t}} = \eta^{self} \cdot \boldsymbol{E^{ev}_{p,t-1}} \cdot (1 - \alpha_{p,t}) + (\eta^{ch} \cdot \boldsymbol{\dot{E}^{ev,+}_{p,t}} - \frac{1}{\eta^{dis}} \cdot \boldsymbol{\dot{E}^{ev,-}_{p,t}}) \cdot dt_p \qquad \forall p \in \mathrm{P}, \quad \forall t \in \mathrm{T} \tag{3c}$$

Beside the electricity balances, Equations 4a to 4f are applied to ensure the feasibility of the solutions. The charging and discharging power of the EVs is upper bounded by the maximum charging and discharging power of the substations connected to the EVs (Eq. 4a and 4b). Then, the state of charge (**SoC**) of the EVs is constrained between 20% and 80% (Eq. 4c to 4e). The reason is to limit rapid aging of the batteries with excessively high or low SoC. In addition, a SoC of 80% at 4 am is asked to ensure the availability of the cars early in the morning. In the case where the EVs are not providing grid services, the discharge power $\dot{E}^{ev,-}$ is set to 0. Therefore, the discharging only comes from the EVs travels and the self-discharge.

$$\boldsymbol{\dot{E}^{ev,-}_{p,t}} \leq \dot{E}^{station,-} \qquad \forall p \in \mathrm{P}, \quad \forall t \in \mathrm{T} \tag{4a}$$

$$\boldsymbol{\dot{E}^{ev,+}_{p,t}} \leq \dot{E}^{station,+} \qquad \forall p \in \mathrm{P}, \quad \forall t \in \mathrm{T} \tag{4b}$$

$$SoC_{min} \leq \frac{\boldsymbol{E^{ev}_{p,t}}}{E^{ev,cap}} \leq SoC_{max} \qquad \forall p \in \mathrm{P}, \quad \forall t \in \mathrm{T} \tag{4c}$$

$$SoC_{min} \leq \frac{\boldsymbol{E^{ev,out}_{p,t}}}{E^{ev,cap} \cdot \alpha_{p,t}} \leq SoC_{max} \qquad \forall p \in \mathrm{P}, \quad \forall t \in \mathrm{T} \tag{4d}$$

$$SoC_{min} \leq \frac{\boldsymbol{E^{ev,in}_{p,t}}}{E^{ev,cap} \cdot (1 - \alpha_{p,t})} \leq SoC_{max} \qquad \forall p \in \mathrm{P}, \quad \forall t \in \mathrm{T} \tag{4e}$$

$$\frac{\boldsymbol{E^{ev}_{p,t=4am}}}{E^{ev,cap}} = SoC_{max} \qquad \forall p \in \mathrm{P} \tag{4f}$$

The last set of constraints are the cyclicity constraints (Eq. 5a and 5b). They prevent the accumulation of electricity in the EVs between the periods by linking the first and last state of the EVs.

$$\boldsymbol{E^{ev,out}_{p,t=1}} = \eta^{self} \cdot \boldsymbol{E^{ev}_{p,t=24}} \cdot \alpha_{p,t=1} - E^{ev,displ.}_{p,t=1} \qquad \forall p \in \mathrm{P} \tag{5a}$$

$$\boldsymbol{E^{ev,in}_{p,t=1}} = \eta^{self} \cdot \boldsymbol{E^{ev}_{p,t=24}} \cdot (1 - \alpha_{p,t=1}) + (\eta^{ch} \cdot \boldsymbol{\dot{E}^{ev,+}_{p,t=1}} - \frac{1}{\eta^{dis}} \cdot \boldsymbol{\dot{E}^{ev,-}_{p,t=1}}) \cdot dt_p \qquad \forall p \in \mathrm{P} \tag{5b}$$

2.4. Key performance indicators

Several key performance indicators (**KPI**) are used to assess the performances of the model. The self-consumption (**SC**) is the share of the onsite generated electricity being consumed within the district. The self-sufficiency (**SS**) corresponds to the share of the electricity demand being supplied by the onsite generated electricity. The PV penetration (**PVP**) is the proportion of the electricity demand that could be supplied by the onsite generated electricity with a SC of 100%. Finally, the global warming potential (**GWP**) accounts for both the construction and operation emissions as described in [23].

$$\mathrm{SC} = (E^{site,+} - E^{tr,-})/(E^{site,+}) \tag{6a}$$

$$\mathrm{SS} = (E^{site,+} - E^{tr,-})/(E^{site,+} - E^{tr,-} + E^{tr,+}) \tag{6b}$$

$$\mathrm{PVP} = E^{site,gen}/(E^{site,+} - E^{tr,-} + E^{tr,+}) \tag{6c}$$

$$\mathrm{G}^{op} = \sum_{\substack{p \in P \\ t \in T}} \left(g^{el,TR}_{p,t} \cdot (E^{tr,+} - E^{tr,-}) + \sum_{b \in B} g^{ng}_{p,t} \cdot H^{gr,+}_{b,p,t} \right) \tag{6d}$$

2.5. Case Study

2.5.1. Input data for the district

The case study considered is a typical central European, sub urban and residential district. It encompasses 31 multi-family and single-family buildings and is located in the climatic zone of Geneva, Switzerland. For the

domestic hot water, typical profiles according to national standard norms are considered [25]. Space heating demand is modelled based on the 1R1C model detailed by [26]. The uncontrollable load profiles are disaggregated from measurements by Holwerger et al. [27].

Ten typical periods and two extreme periods are identified using k-medoids clustering to represent the weather data time series. In addition to global irradiation and ambient temperature, the typical periods are differentiated between weekdays and weekends in order to consider the difference of plug-out profiles. The time horizon is 20 years and the interest rate is 2%. The electricity retail tariff is fixed to 0.2 CHF/kWh and the feed-in tariff is 0.08 CHF/kWh. The sources for the buildings, units and weather data are further detailed by Middelhauve [23].

2.5.2. Input data for electric vehicles

The input parameters for the EVs model come from two main sources. First, a detailed analysis on traveling habits has been performed by the Swiss government, Federal Office of Statistic (FSO) [28]. Second, Calearo et al. released a review on data estimations for EVs modeling [29]. From these sources, the following parameters were estimated. The daily travel by car is fixed to 23.8 $\frac{km}{person \cdot day}$ [28]. With an occupancy of 1.56 $\frac{person}{car}$ [28] and a running distance of 6 $\frac{km}{kWh}$ [29], the electricity consumption reaches 6.2 $\frac{kWh}{car \cdot day}$. The plug-out profiles are based on the profiles by FSO [28]. In addition, French and German government data are used to extrapolate the plug-out profiles during the weekends based on the method by Schnidrig [30]. The plug-out profiles set in the model are shown on Figure 1. The International Energy Agency [31] estimates that the share of EVs should reach 20% by 2030 and 60 % by 2040. This study applies the objective of 20% EV integration corresponding to 30 EVs. The maximum charging and discharging power of substations is set to 11 $\frac{kW}{car}$ [29]. The charging and discharging efficiencies are both set to 90% [32] and the self-discharge rate is 99.992% [32]. The battery capacity of each EV is set to 70 kWh since they are between 40 and 70 kWh in 2022 and are expected to reach between 70 and 80 kWh in 2030 [29].

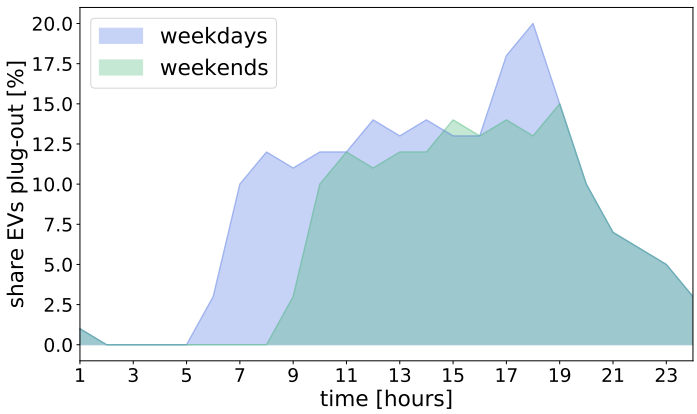

Figure 1: Considered plug-out profile of the EVs that are based on data provided by FSO [28].

3. Results and Discussion

The results and discussion aim at demonstrating the feasibility of the EVs integration within the renewable energy hub and its potential to offer service to the grid. First, the results are quantified in terms of costs, associated GWP and usage of onsite generated electricity. A special focus is given on the energy system design of the renewable energy hub and its influence on the operating cost to charge the EVs. Second, the management of the onsite generated electricity is analysed to highlight synergies between the PV and EV units. Finally, the EVs integration considering the power grid limits is discussed.

3.1. Cost analysis of the EVs integration in the renewable energy hub

Among the most popular EV services to the grid (V2G) are peak-shaving, load levelling, active power reserves and renewable integration supports. Figure 2 compares the performances of two control strategies with respect to a third system without EVs integration. To draw comparisons, the same PV capacity has been set for each scenario. This capacity corresponds to the PV capacity installed with the minimum TOTEX of the energy system without EVs (0.025 kW_p/m^2). The sizes of the other energy conversion units and the operation of the energy system are kept as decision variables. The additional electricity demand from the bidirectional EVs resulted in an OPEX increase by 11%, whereas the unidirectional one increased the OPEX by 18%. This is

explained by the high SC of 70% obtained with the bidirectional control. Compared to unidirectional control and to the case without EVs, the SC increased by 13% and 27% respectively. While the PV capacity is the same between the three scenarios, the PVP decreases with the integration of EVs due to the additional electricity demand. Only the bidirectional control can enhance the SS of the system. Even if the unidirectional control increases the SC, it only compensates the drop of PVP. The electricity demand from the EVs increases the GWP by 6% and 9%. Even if the increase is marginal, the GWP impact of the EV integration with unidirectional control remains 50% higher compared to the bidirectional one.

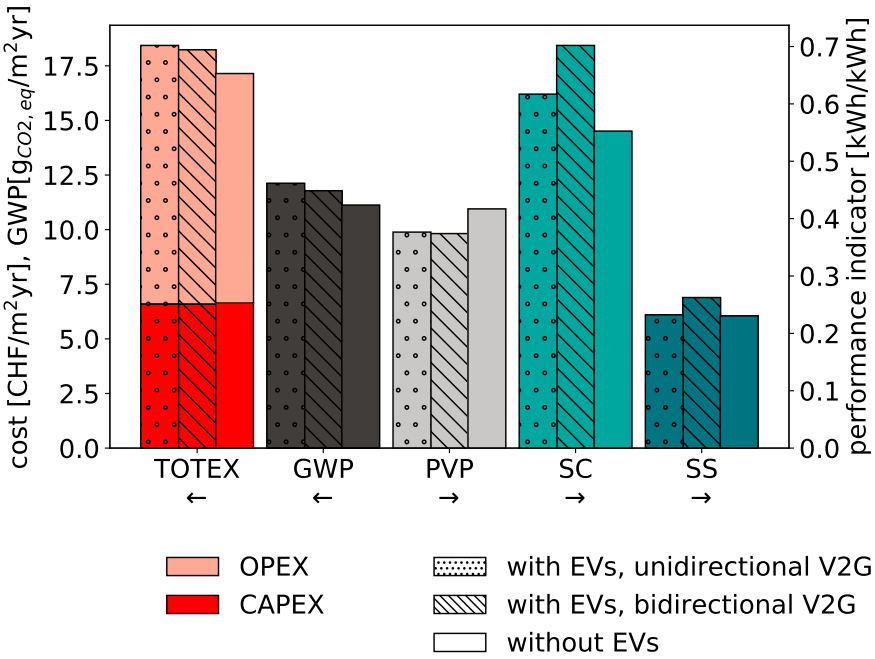

Figure 2: Solutions for the minimum of the objective function TOTEX. The KPIs are evaluated for three scenarios: without EVs integration and with integration with two different control strategies. The arrow below each column indicates which axis to look at for each KPI. The bidirectional V2G integration of the EVs enhanced the SC from 57% to 70%.

Since the TOTEX minimization represents only one optimal solution, a MOO is performed with the OPEX and CAPEX as objective functions. Figure 3 shows the CAPEX breakdown and OPEX for each solution of the pareto front. Both scenarios with and without EVs integration are considered. The control strategy is the bidirectional one. At low CAPEX scenarios, gas boilers were installed. The system did not generate any renewable electricity and the EVs charging was relying completely on the power grid, which resulted in the maximum of charging costs (1.6 CHF/m^{2}yr). Increasing CAPEX allowed decreasing OPEX by investments into heat pumps and PV panels. The presence of cheap electricity in the district decreased the OPEX of the EVs, which reached the minimal value at 0.5 CHF/m^{2}yr corresponding to a 70% decrease. At the highest CAPEX, the PV capacity is maximal, batteries are installed and the OPEX is negligible or even negative, due to feed-in compensations. In these scenarios, the OPEX of the EVs increased to 1 CHF/m^{2}yr due to the competition with heat pumps, which also maximize the SC of electricity. Also batteries provide an alternative to the EVs to increase the SC. For each scenario, the investment decisions are unchanged by the integration of EVs. The additional demand is integrated by only adapting the operation. It should be mentioned that a 20%-share of electric mobility was considered. It is probable that a higher share would change the investment decisions.

3.2. Management of the onsite generated electricity and service to the grid

In the following, the renewable energy use and the EV operation management are discussed to understand how the renewable energy hub adapts its operation to integrate EVs. The breakdown of the renewable energy use is detailed in Figure 4 with respect to the PV capacity installed in the district. The annual electricity generation from PV panels is given by the dashed black line. The light red area corresponds to the share of this electricity being sold to the grid, the rest being self-consumed. All values are calculated with the bidirectional control of EVs except for the dashed red line corresponding to the electricity annual exports without EVs integration.

Around 25% of the renewable energy was directly self-consumed by the building where the PV units are installed. Then, between 9% to 13% of the electricity was exported by the buildings and directly consumed by

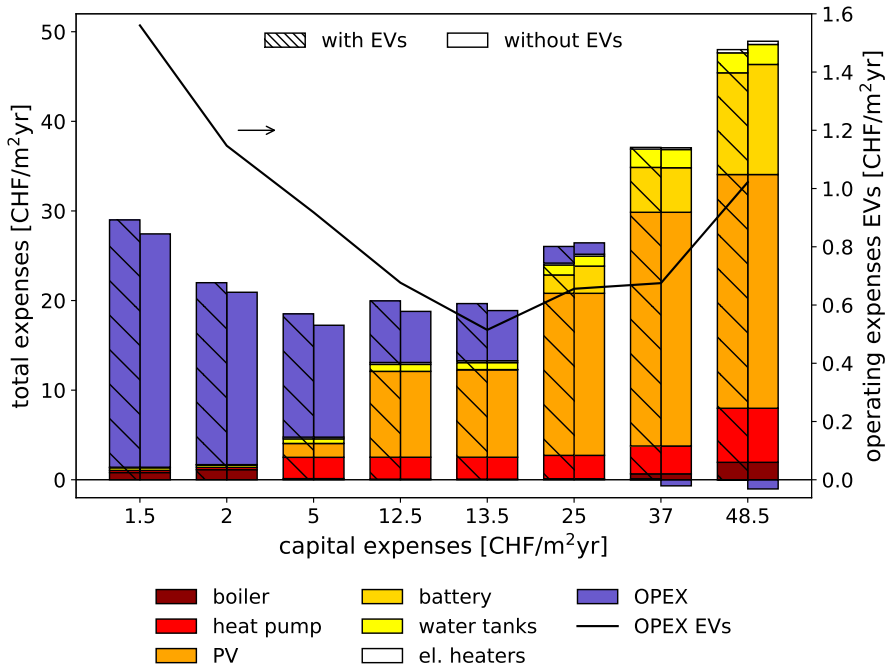

Figure 3: Capital cost breakdown and operating costs of the MOO. The EVs integration changed the operation decisions and not the investment decisions. The charging operating costs could be decreased by 70% with the self-consumption of renewable energy.

a neighbor within the district. These electricity re-imports represent the benefit of the district scale consideration. The share of the onsite generated electricity that was consumed by the EVs reached around 4%. This additional demand lies within the export region of the system without EVs. It means that the EVs mainly self-consumed electricity that should have been sold to the grid. In addition, at low PV capacity, they also provided renewable integration support by increasing the share of re-imports in the district. Above the PV capacity of 0.15 kW_p/m^2, a part of the EVs electrical demand was supplied by electricity that would have been self-consumed. It happened when stationary batteries were installed and created a competition for SC.

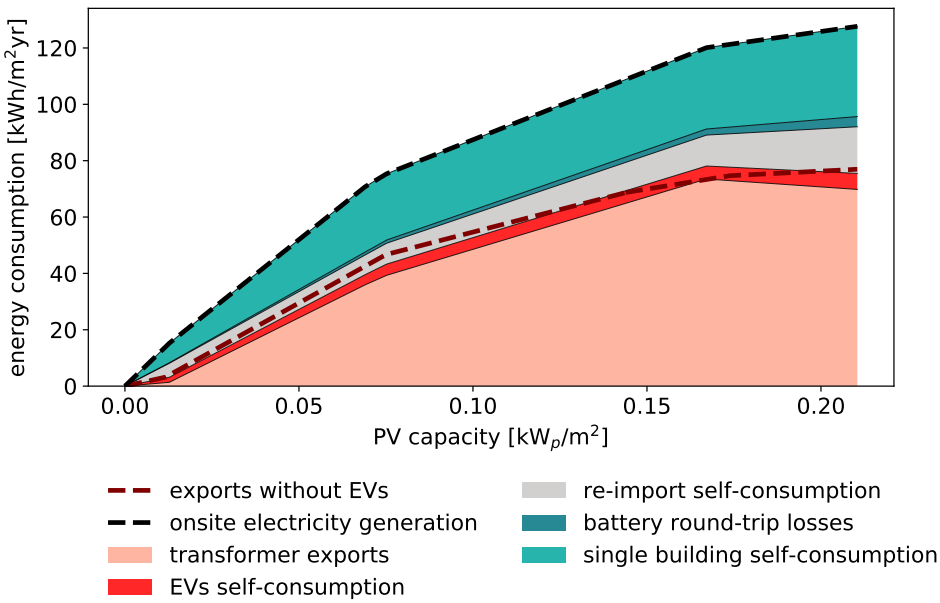

Figure 4: Breakdown by usage of the annual renewable energy generation from PV panels with EVs integration. The annual renewable electricity exports without EVs integration is shown by the red dashed line. Most of the renewable energy used to charge the EVs is taken from electricity that would have been sold to the grid.

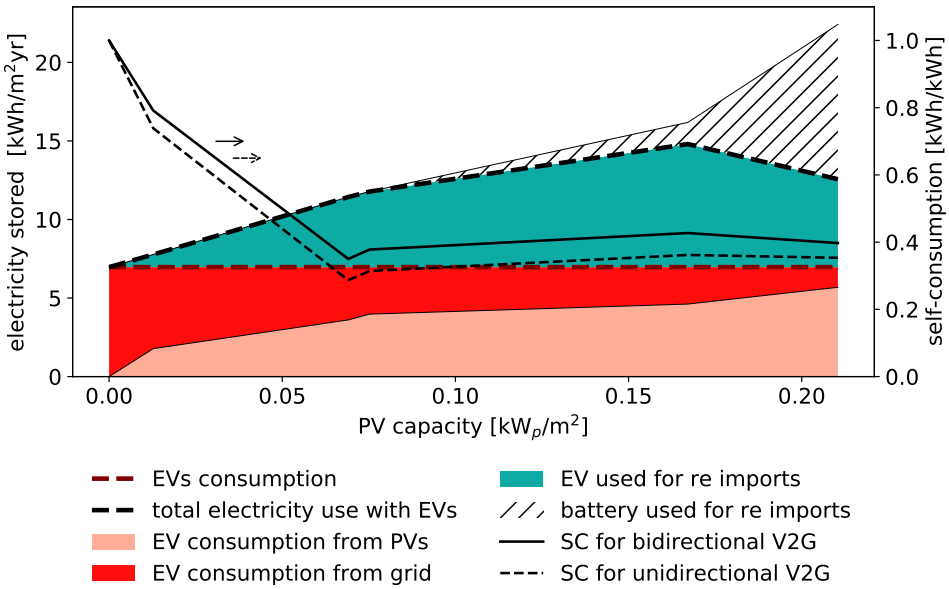

Figure 5: Breakdown of the energy stored in the EVs and SC of the renewable energy hub. The energy stored in stationary batteries is as well shown to evaluate the overall electricity storage. Up to 82% of the EVs electricity consumption could be supplied by renewable energy.

Figure 5 provides a deeper analysis on the role of EVs to supply grid services by showing the annual electricity use that is stored in the EVs. The annual EV demand for mobility corresponds to 7 kWh/m^{2}yr. Along with the PV capacity increase, the share of renewable electricity consumed in the EVs increased to 82%. Between a PV capacity of 0.07 and 0.2 kW$_p$/m^2 around 50% of the energy stored in the EVs was used for re-imports within the district. These active power reserves increased the SC of the renewable energy hub by 11% to 17%. While the PV capacity increased, the SC decreased due to the difficulties to store the excess renewable energy when the electricity demand is low. Then, it reached a plateau at around 40%. In parallel, stationary batteries are installed which reduced the contributions of the EVs to re-imports. The batteries provide a SC support to store the onsite generated electricity while the EV storage capacity in the district is low.

3.3. Electric mobility grid integration

The consideration of the grid constraint during the integration of EVs is crucial since the additional electricity demand might overload the transformer capacity. Figure 6 shows the load duration curve at the transformer level for three scenarios. The first one is the current energy system without EVs. It is obtained with a TOTEX minimization. The system contains heat pumps and PV panels and the transformer capacity is respected. The integration of EVs within this system exceeds the transformer capacity by 200 kW for 200 hours within the year. Even if the EVs integration increases the SC, it is not sufficient to respect the transformer capacity. This implies that a grid-unaware integration of EVs threaten the electricity security of supply for the district. To consider the grid limitations, the transformer capacity constraint (Eq. 2a) is applied to obtain a feasible integration of EVs. The constraint increased the TOTEX by 4% mainly coming from the installation of a stationary battery. This additional storage capacity enhanced the SC to 78%, representing a SC increase by 11%. Both imports and exports were better scheduled by the peak shaving and by load levelling. This demonstrates the importance to consider the renewable energy hub at the district scale in order to apply grid constraints during the optimization.

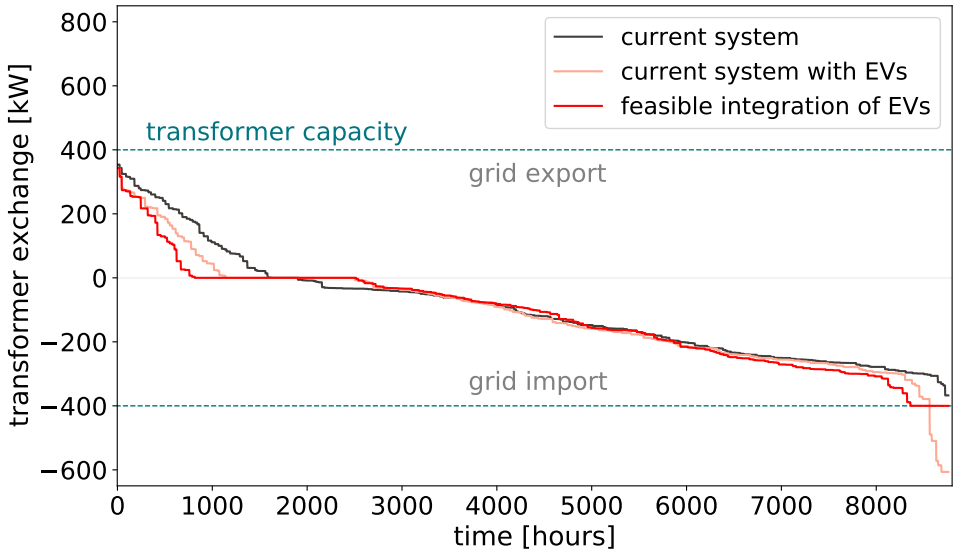

Figure 6: Load duration curve of the system without EVs integration, with EVs integration but without grid constraint and with EVs integration and grid constraint. Without a grid-aware integration, the EVs generate power shortage during 200h per year

4. Conclusion

The objective of this paper was to demonstrate the grid service potential and the grid impact of electric vehicles in a renewable energy hub at the district scale. The latter was built with a multi-energy and grid-aware framework. The EVs were modelled at the district scale as controllable storage capacities offering grid services. The charging control strategy was a bidirectional smart control. Multi-objective optimization was performed to analyse the investment and operation decisions. The main outcomes are listed below.

- At the minimum total costs, the electric mobility increased the self-consumption of renewable electricity from 57% to 70%. Compared to purchasing electricity from the grid, this high self-consumption reduced the charging costs by 70%.
- The investment decisions within the renewable energy hub were unchanged by the integration of a 20%-share of electric mobility. The most economic choice was to satisfy the additional electricity demand by self-consuming the onsite generated electricity sold to the grid.
- Up to 82% of the additional electricity demand from EVs could be supplied by renewable energy.
- With a 20%-share of electric mobility the low-voltage transformer in the district showed a capacity shortage during 200 hours per year. Applying the grid constraint reduced the maximum of the imports by increasing the SC and by load levelling.

The presented results contribute to a better understanding of electric mobility integration in renewable energy hubs with an optimal interconnection of multiple energy carriers. This holistic approach allows the consideration of synergies that would be difficult to determine using an aggregated or a pre-selected model. The possible extension of the presented work is to model future scenarios with an increased share of electric mobility. This analysis allows useful insights of the potential and limitations of grid-aware integration of EVs and the opportunities to enhance renewable energy integration by further exploiting service to the grid.

References

[1] Internation Renewable Energy Agency. World Energy Transitions Outlook. 2021.

[2] Intergovernmental panel on climat change. *Climate Change 2014: Mitigation of Climate Change*. Cambridge, UK ; New York, 2014.

[3] Robert C. Green, Lingfeng Wang, and Mansoor Alam. The impact of plug-in hybrid electric vehicles on distribution networks: A review and outlook. *Renewable and Sustainable Energy Reviews*, 15(1):544–553, January 2011.

[4] David B. Richardson. Electric vehicles and the electric grid: A review of modeling approaches, Impacts, and renewable energy integration. *Renewable and Sustainable Energy Reviews*, 19:247–254, March 2013.

[5] Junjie Hu, Hugo Morais, Tiago Sousa, and Morten Lind. Electric vehicle fleet management in smart grids: A review of services, optimization and control aspects. *Renewable and Sustainable Energy Reviews*, 56:1207–1226, April 2016.

[6] Kang Miao Tan, Vigna K. Ramachandaramurthy, and Jia Ying Yong. Integration of electric vehicles in smart grid: A review on vehicle to grid technologies and optimization techniques. *Renewable and Sustainable Energy Reviews*, 53:720–732, January 2016.

[7] Nico Brinkel, Tarek AlSkaif, and Wilfried van Sark. Grid congestion mitigation in the era of shared electric vehicles. *Journal of Energy Storage*, 48:103806, April 2022.

[8] Lena-Marie Ritte, Stefan Mischinger, Kai Strunz, and Johannes Eckstein. Modeling photovoltaic optimized charging of electric vehicles. In *2012 3rd IEEE PES Innovative Smart Grid Technologies Europe (ISGT Europe)*, pages 1–8, Berlin, Germany, October 2012. IEEE.

[9] Xiaohua Wu, Xiaosong Hu, Yanqiong Teng, Shide Qian, and Rui Cheng. Optimal integration of a hybrid solar-battery power source into smart home nanogrid with plug-in electric vehicle. *Journal of Power Sources*, 363:277–283, September 2017.

[10] Bo Wang, Payman Dehghanian, and Dongbo Zhao. Chance-Constrained Energy Management System for Power Grids With High Proliferation of Renewables and Electric Vehicles. *IEEE Transactions on Smart Grid*, 11(3):2324–2336, May 2020.

[11] Katrin Seddig, Patrick Jochem, and Wolf Fichtner. Integrating renewable energy sources by electric vehicle fleets under uncertainty. *Energy*, 141:2145–2153, December 2017.

[12] Xuan Hou, Jun Wang, Tao Huang, Tao Wang, and Peng Wang. Smart Home Energy Management Optimization Method Considering Energy Storage and Electric Vehicle. *IEEE Access*, 7:144010–144020, 2019.

[13] Auyon Chakrabarti, Rafael Proeglhoef, Gonzalo Bustos Turu, Romain Lambert, Arthur Mariaud, Salvador Acha, Christos N. Markides, and Nilay Shah. Optimisation and analysis of system integration between electric vehicles and UK decentralised energy schemes. *Energy*, 176:805–815, June 2019.

[14] N.B.G. Brinkel, W.L. Schram, T.A. AlSkaif, I. Lampropoulos, and W.G.J.H.M. van Sark. Should we reinforce the grid? Cost and emission optimization of electric vehicle charging under different transformer limits. *Applied Energy*, 276:115285, October 2020.

[15] Joao Soares, Marco Silva, Bruno Canizes, and Zita Vale. MicroGrid DER control including EVs in a residential area. In *2015 IEEE Eindhoven PowerTech*, pages 1–6, Eindhoven, Netherlands, June 2015. IEEE.

[16] Tianyang Zhang, Chi-Cheng Chu, and Rajit Gadh. A two-tier energy management system for smart electric vehicle charging in UCLA: A Solar-To-Vehicle (S2V) case study. In *2016 IEEE Innovative Smart Grid Technologies - Asia (ISGT-Asia)*, pages 288–293, Melbourne, Australia, November 2016. IEEE.

[17] S. Bracco, C. Cancemi, F. Causa, M. Longo, and S. Siri. Optimization model for the design of a smart energy infrastructure with electric mobility. *IFAC-PapersOnLine*, 51(9):200–205, 2018.

[18] Raji Atia and Noboru Yamada. More accurate sizing of renewable energy sources under high levels of electric vehicle integration. *Renewable Energy*, 81:918–925, September 2015.

[19] Portia Murray, Jan Carmeliet, and Kristina Orehounig. Multi-Objective Optimisation of Power-to-Mobility in Decentralised Multi-Energy Systems. *Energy*, 205:117792, August 2020.

[20] Moritz Mittelviefhaus, Giacomo Pareschi, James Allan, Gil Georges, and Konstantinos Boulouchos. Optimal investment and scheduling of residential multi-energy systems including electric mobility: A cost-effective approach to climate change mitigation. *Applied Energy*, 301:117445, November 2021.

[21] Stefan Englberger, Kareem Abo Gamra, Benedikt Tepe, Michael Schreiber, Andreas Jossen, and Holger Hesse. Electric vehicle multi-use: Optimizing multiple value streams using mobile storage systems in a vehicle-to-grid context. *Applied Energy*, 304:117862, December 2021.

[22] Quentin Hoarau and Yannick Perez. Interactions between electric mobility and photovoltaic generation: A review. *Renewable and Sustainable Energy Reviews*, 94:510–522, October 2018.

[23] Luise Middelhauve. *On the role of districts as renewable energy hubs*. PhD thesis, EPFL, 2022.

[24] Paul Michael Stadler. *Model-based sizing of building energy systems with renewable sources*. PhD thesis, EPFL, 2019.

[25] SIA. 2024:2025 Raumnutzungsdaten fur die Energie- und Gebaudetechnik. *Schweizerischer Ingenieur und Architektenverein*, 2015.

[26] Luc Girardin. *A GIS-based Methodology for the Evaluation of Integrated Energy Systems in Urban Area*. PhD thesis, EPFL, 2012.

[27] Jordan Holweger, Marina Dorokhova, Lionel Bloch, Christophe Ballif, and Nicolas Wyrsch. Unsupervised algorithm for disaggregating low-sampling-rate electricity consumption of households. *Sustainable Energy, Grids and Networks*, 19:100244, September 2019.

[28] Federal office of statistic. Comportement de la population en matière de transports. Technical Report 841-1500, Neuchâtel, 2017.

[29] Lisa Calearo, Mattia Marinelli, and Charalampos Ziras. A review of data sources for electric vehicle integration studies. *Renewable and Sustainable Energy Reviews*, 151:111518, November 2021.

[30] Jonas Schnidrig. *Assessment of green mobility scenarios on European energy systems*. PhD thesis, EPFL, 2020.

[31] Internation Energy Agency. Net Zero by 2050 - A Roadmap for the Global Energy Sector. page 224, 2021.

[32] Frauke Oldewurtel, Andreas Ulbig, Manfred Morari, and Goran Andersson. Building control and storage management with dynamic tariffs for shaping demand response. In *2011 2nd IEEE PES International Conference and Exhibition on Innovative Smart Grid Technologies*, pages 1–8, Manchester, United Kingdom, December 2011. IEEE.